Received: 26 September 2022 | Revised: 27 December 2022 | Accepted: 4 January 2023

DOI: 10.1002/alz.12975

Alzheimer's & Dementia®
THE JOURNAL OF THE ALZHEIMER'S ASSOCIATION

RESEARCH ARTICLE

Anatomical MRI staging of frontotemporal dementia variants

Vincent Planche[1,2] | **Boris Mansencal**[3] | **José V. Manjon**[4] | **Thomas Tourdias**[5,6] | **Gwenaëlle Catheline**[7] | **Pierrick Coupé**[3] | **For the Frontotemporal Lobar Degeneration Neuroimaging Initiative and the National Alzheimer's Coordinating Center cohort**

[1]Univ. Bordeaux, CNRS, UMR 5293, Institut des Maladies Neurodégénératives, Bordeaux, France

[2]Centre Mémoire Ressources Recherches, Pôle de Neurosciences Cliniques, CHU de Bordeaux, Bordeaux, France

[3]CNRS, Univ. Bordeaux, Bordeaux INP, Talence, France

[4]Instituto de Aplicaciones de las Tecnologías de la Información y de las Comunicaciones Avanzadas (ITACA), Universitat Politècnica de València, Valencia, Spain

[5]Inserm U1215 - Neurocentre Magendie, Bordeaux, France

[6]Service de Neuroimagerie diagnostique et thérapeutique, CHU de Bordeaux, Bordeaux, France

[7]Univ. Bordeaux, CNRS, UMR 5287, Institut de Neurosciences Cognitives et Intégratives d'Aquitaine, Bordeaux, France

Correspondence
Vincent Planche, Institut des Maladies Neurodégénératives, UMR CNRS 5293, Centre Broca Nouvelle-Aquitaine, 146 rue Léo Saignat – 33076 Bordeaux cedex, France.
Email: vincent.planche@u-bordeaux.fr

Funding information
French National Research Agency (ANR-18-CE45-0013); Laboratory of Excellence TRAIL ANR-10-LABX-57; Investments for the future Program IdEx Bordeaux (ANR-10-IDEX-03-02 and RRI "IMPACT"); Spanish Ministerio de Ciencia e innovación (PID2020-118608RB-I00)

Abstract

INTRODUCTION: The three clinical variants of frontotemporal dementia (behavioral variant [bvFTD], semantic dementia, and progressive non-fluent aphasia [PNFA]) are likely to develop over decades, from the preclinical stage to death.

METHODS: To describe the long-term chronological anatomical progression of FTD variants, we built lifespan brain charts of normal aging and FTD variants by combining 8022 quality-controlled MRIs from multiple large-scale data-bases, including 107 bvFTD, 44 semantic dementia, and 38 PNFA.

RESULTS: We report in this manuscript the anatomical MRI staging schemes of the three FTD variants by describing the sequential divergence of volumetric trajectories between normal aging and FTD variants. Subcortical atrophy precedes focal cortical atrophy in specific behavioral and/or language networks, with a "radiological" prodromal phase lasting 8–10 years (time elapsed between the first structural alteration and canonical cortical atrophy).

DISCUSSION: Amygdalar and striatal atrophy can be candidate biomarkers for future preclinical/prodromal FTD variants definitions.

KEYWORDS
atrophy, frontotemporal dementia, lifespan, MRI, primary progressive aphasia, semantic dementia, staging

Highlights

- We describe the chronological MRI staging of the most affected structures in the three frontotemporal dementia (FTD) syndromic variants.
- In behavioral variant of FTD (bvFTD): bilateral amygdalar, striatal, and insular atrophy precedes fronto-temporal atrophy.
- In semantic dementia: bilateral amygdalar atrophy precedes left temporal and hippocampal atrophy.
- In progressive non-fluent aphasia (PNFA): left striatal, insular, and thalamic atrophy precedes opercular atrophy.

1 | INTRODUCTION

Frontotemporal dementia (FTD) is a group of clinical syndromes characterized by progressive impairments in language and/or executive functions and/or behavior. This umbrella term includes the behavioral variant of FTD (bvFTD) and two distinct forms of primary progressive aphasia: semantic dementia and progressive non-fluent aphasia (PNFA). Apart from the genetic forms (for which the diagnosis of certainty can be provided by molecular biology), the diagnosis of FTD is challenging because there are many psychiatric or neurological differential diagnoses and no specific pathological biomarker.[1] Moreover, the early stages of sporadic FTD are still poorly characterized and research criteria for prodromal bvFTD have only been proposed in 2022,[2] and are still lacking for semantic dementia and PNFA. The definition of these preclinical and prodromal stages of FTD variants is however crucial in the prospect of future therapeutic actions, as illustrated by the development of disease-modifying therapies specifically in prodromal Alzheimer's disease.[3]

The value of anatomical MRI for diagnosing FTD is well-established and it is included in current diagnostic criteria. Indeed, the location of maximal atrophy within behavioral and/or language neural networks is supposed to determine the clinical presentation of FTD variants.[4] Frontal and/or insular and/or anterior temporal atrophy (or hypometabolism on FDG-PET) is, for instance, a mandatory criterion to achieve the "probable" level of a bvFTD diagnosis.[5] Regarding the diagnosis of primary progressive aphasia variants, predominant anterior temporal lobe atrophy will support the diagnosis of semantic dementia on top of clinical diagnosis, and predominant left posterior fronto-insular atrophy is an imaging support for the diagnosis of PNFA.[6]

These anatomical descriptions of typical focal atrophy in FTD variants are mainly based on subjects at the late dementia stages, with advanced cortical atrophy.[7,8] However, brain structural alterations precede symptoms onset in neurodegenerative diseases and MRI studies in presymptomatic carriers of FTD-causative mutations (*MAPT*, *GRN*, or *C9orf72*) reported brain atrophy up to 20 years before symptoms onset.[9,10,11,12] The chronological anatomical progression of FTD variants from the preclinical stage to death has never been documented in the more common sporadic forms of FTD. Providing insights into the spatiotemporal spreading of brain atrophy is therefore crucial to better understand the early pathophysiological process underlying FTD, and to develop future imaging-supported diagnostic criteria for preclinical or prodromal FTD variants. Structural brain imaging can also help to provide evidence of disease-course modification in future clinical trials, as it can explain a substantial portion of variance in clinical measures.[13]

In this study, we propose to depict the progressive anatomical staging of FTD variants. Because cohorts of sporadic FTD patients with longitudinal imaging data over decades – from the preclinical stage to death – are not available, we took advantage of BigData sharing in neuroimaging, combined with lifespan modeling of brain volume changes[14] (also known as *brain charts*[15]), to quantify disease-related changes. These extrapolated dynamic volumetric trajectories based on cross-sectional MRI have been previously validated using "truly" longitudinal data in order to describe the MRI staging of brain atrophy progression in Alzheimer's disease.[16] In the present study, the progressive pattern of neuroanatomical variations across all three subtypes of FTD (107 bvFTD, 44 semantic dementia, and 38 PNFA) was compared to brain charts built from 8022 MRI of healthy controls at different ages and covering the entire lifespan.

RESEARCH IN CONTEXT

1. **Systematic review**: The authors reviewed the literature using traditional sources. The location of maximal atrophy within behavioral and/or language neural networks determine the clinical presentation of frontotemporal dementia (FTD) variants. Typical atrophy patterns at the dementia stage are reported in diagnostic criteria of behavioral variant FTD (bvFTD), semantic dementia, and progressive non-fluent aphasia (PNFA).
2. **Interpretation**: This study is the first to use lifespan brain charts of normal aging and FTD variants to provide information about the onset and progression of the three clinical presentations of FTD. The authors identify five major stages of atrophy progression in each FTD variant, whereby subcortical atrophy precedes the canonical atrophy pattern by 8–10 years.
3. **Future directions**: The description of these progressive structural MRI staging schemes is of major interest in the understanding of FTD variants pathophysiology, and in the development of future prodromal diagnostic criteria for bvFTD, semantic dementia, and PNFA.

2 | METHODS

2.1 | Standard protocol approvals, registrations, and patient consents

All data were obtained in deidentified format upon request from external study centers, who ensured compliance with ethical guidelines. All subjects included in the MRI databases used in this study provided informed consent. The protocol for each study/cohort was approved by the institution review board at all sites (see the Acknowledgments section).

2.2 | Datasets

Normal and FTD variants trajectories of brain volumes were estimated thanks to the aggregation of 23 open access MRI databases. We used a total of 8211 T1-weigthed MRIs collected on 1.5T or

TABLE 1 Datasets description and clinical characteristics of patients.

	Healthy controls	Frontotemporal dementia		
		bvFTD	Semantic dementia	PNFA
No. of subjects	8022	107 (70 NIFD; 37 NACC)	44 (37 NIFD; 7 NACC)	38 (34 NIFD; 4 NACC)
Age (years),mean [range]	40.0 [0.7–100.2]	62.4 [35.1–76.3]	63.9 [50–85.2]	68.3 [54–81]
Gender	F = 4097; M = 3923	F = 38; M = 69	F = 20; M = 24	F = 22; M = 16
Global FTLD-CDR				
<1		32.4%	63.6%	81.6%
≥1		67.6%	36.4%	18.4%
FTLD-CDR-sb, mean(SD)	–	6.13 (3.5)	3.9 (1.9)	2.2 (1.9)
MoCA, mean (SD)	–	19.5 (5.7)	16.5 (6.1)	19.5 (6.7)

Abbreviations: bvFTD: behavioral variant frontotemporal dementia; FTLD-CDR: Frontotemporal lobar degeneration modified Clinical Dementia Rating scale (a global score ≥1 indicate the stage of dementia); FTLD-CDR-sb: FTLD-CDR sum of boxes; MoCA: Montreal Cognitive Assessment; NACC: National Alzheimer's Coordinating Center; NIFD: Frontotemporal Lobar Degeneration Neuroimaging initiative; PNFA: progressive non-fluent aphasia; SD, standard deviation.

3T magnets. After quality control (see below), 8022 MRIs from healthy subjects, covering the entire lifespan (from 1 to 100 years of age) were included in the study. The 23 cohorts with healthy subjects were: *C-MIND* (*n* = 236, https://research.cchmc.org/c-mind/), *NDAR* (*n* = 382, ndar.nih.gov), *ABIDE* (*n* = 492 ht tps://fcon_1000.projects.nitrc.org/indi/abide/), *ICBM*: (*n* = 294 https://www.loni.usc.edu/ICBM/), *IXI* (*n* = 549, http://brain-development.org/ixi-dataset/), *ADNI1&2* (*n* = 404, ht tps://adni.loni.usc.edu), *AIBL* (*n* = 467, www.aibl.csiro.au/), ADHD-200 (*n* = 544, ht tps://fcon_1000.projects.nitrc.org/indi/adhd200/), DLBS (*n* = 315, ht tps://fcon_1000.projects.nitrc.org/indi/retro/dlbs.html), ISYB (*n* = 213, https://www.scidb.cn/en/detail?dataSetId = 826407529641672704), MIRIAD (*n* = 23, https://www.ucl.ac.uk/drc/research/research-methods/minimal-interval-resonance-imaging-alzheimers-disease-miriad), PPMI (*n* = 166, https://www.ppmi-info.org/), PREVENT-AD (*n* = 307, ht tps://openpreventad.loris.ca/), Amsterdam open MRI collection (AOMIC_ID100 & PIOP1 & PIOP2, *n* = 1361, ht tps://nilab-uva.github.io/AOMIC.github.io/), Calgary cohort (*n* = 267, h ttps://osf.io/axz5r/), CamCAN (*n* = 653, ht tps://camcan-archive.mrc-cbu.cam.ac.uk/dataaccess/), PIXAR (*n* = 155, https://openneuro.org/datasets/ds002228/versions/1.1.0), SALD (*n* = 494, ht tps://fcon_1000.projects.nitrc.org/indi/retro/sald.html), SRPBS (*n* = 791, https://bicr-resource.atr.jp/srpbsopen/), NACC (*n* = 161), and NIFD (*n* = 135).

For FTD variants, we pooled MRI from the Frontotemporal Lobar Degeneration Neuroimaging initiative (NIFD, https://4rtni-ftldni.ini.usc.edu/) and the National Alzheimer's Coordinating Center cohort (NACC, https://naccdata.org/data-collection/forms-documentation/ftld-3). All patients with FTD met the international criteria for bvFTD, semantic dementia or PNFA.[5,6] In order to have a population with homogeneous diagnoses, only subjects included after 2011 in the NACC cohort and meeting the new diagnostic criteria for bvFTD or language variants were included in this study. We included 108 bvFTD (107 after quality control), 47 semantic dementia (44 after quality control) and 39 PNFA (38 after quality control) (Table 1 and Figure S1).

2.3 | Image processing

All the considered T1-weighted MRI were processed with AssemblyNet (freely available at https://github.com/volBrain/AssemblyNet)[17] This software produces whole brain segmentation of fine-grained structures using a large ensemble of deep neural networks. AssemblyNet is robust to acquisition protocols, age of subjects, and presence of brain pathology.[17] All the images were preprocessed to homogenize their patterns by setting them into a common geometrical and intensity space. The preprocessing steps started with denoising,[18,19] then the images were corrected for inhomogeneity[20] and affine-registered into the Montreal Neurological Institute (MNI) space using ANTS.[21] Finally a tissue-based intensity normalization was used.[22] For the segmentation process, the intracranial cavity was segmented using DeepICE method.[23] Afterward, structure segmentation was achieved using 250 U-Nets through a multi-scale framework.[17]

All the images were automatically quality controlled using an artificial intelligence-based method RegQCNET.[24] After this first selection, a human-based multi-stage quality control procedure was performed blinded of the subject's group, as previously described.[14,25] A visual assessment was done for all input images by checking screen shots of one sagittal, coronal, and axial slices in the middle of the 3D volume. Images were rejected if partial head coverage, motion artefact, high distortion, or abnormal noise level was detected. Then, a visual assessment of processing quality was carried out using the segmentation report, which provides screenshots for each pipeline step. Images were rejected after this step in case of inaccurate registration in the MNI space, inaccurate intracranial cavity extraction, missing brain structures, or over/under-segmentation of brain structures. A

last control was performed by individually checking all outliers (values higher/lower than two standard deviations of the estimated model). For each outlier, the segmentation map was re-inspected using a 3D viewer. In case of segmentation failure, the subject was removed from the study. A breakdown of cases excluded at each step of the quality control stages is provided in Figure S1.

On the 132 structures produced by AssemblyNet following the Neuromorphometrics labels,[26] we considered the 120 gray matter regions (60 left and 60 right): 9 subcortical structures, 17 frontal gyri/lobules, 8 temporal gyri/lobules, 6 parietal gyri/lobules, 8 occipital gyri/lobules, 6 gyri in the limbic cortex, 5 sub-regions of the insular cortex, and cerebellar gray matter.

2.4 | Statistical analyses

To compensate for the variability introduced by head size difference, models were estimated on normalized volumes (% of total intracranial volume). Moreover, we used z-score of normalized volume to enable comparison between structures of different sizes. The normal distribution of each normalized volume was tested using Kolmogorov-Smirnov test at 95%. Statistics were performed with Matlab using default parameters.

Different strategies were considered to model the trajectories of each brain structure over time, as previously described.[25] Briefly, the candidate models were tested from the simplest to the most complex: (1) a linear model, (2) a quadratic model, and (3) a cubic model. A model was kept as a potential candidate only when simultaneously F-statistic based on analysis of variance (ANOVA; i.e., model vs. constant model) was significant ($p < 0.05$) and when all its coefficients were significant using t-statistic ($p < 0.05$). We finally used the Bayesian Information Criterion (BIC) to compare the candidate models and we selected the model providing the lowest BIC. This model selection procedure was applied to all the considered structures.

Afterward, distances between healthy and FTD variants trajectories were computed on the estimated models. The prediction bounds were estimated with a confidence level of 95%. A brain structure was considered to be significantly smaller in one FTD variant compared to healthy aging when the two structural trajectories diverged and when their 95% confidence intervals no longer overlapped (Figure 1 and Figures S2 and S3). This approach is a conservative version of the *t*-test since the *t*-test can be significant when 95% confidence intervals overlap, while it is always significant when 95% confidence intervals do not overlap.[27] Then, all divergent structures were mapped across time and space on standardized sagittal, coronal and axial MRI planes (upper panels of Figure 2 for bvFTD, Figure 3 for semantic dementia and Figure 4 for PNFA). Finally, the sequence of significant divergence of the most affected brain structures (top 50% of atrophic structures) was listed in chronological order to obtain the MRI staging scheme of each FTD variants (lower panels of Figures 2, 3 and 4).

3 | RESULTS

3.1 | Dataset description

To study the brain volumetric trajectories of healthy controls and the three FTD variants across the entire lifespan, we compiled several open-access databases to construct four datasets. Their composition and characteristics are described in Table 1. The patients with FTD included in the study represented a large spectrum of disease severity, from mild cognitive or behavioral impairment with relatively preserved functional independence (global FTLD-CDR < 1) to dementia (global FTLD-CDR > 1). The mean Montreal Cognitive Assessment (MoCA) ranged from 16.5/30 to 19.5/30 depending on the group, with large standard-deviations (5.7–6.7), also suggesting a wide spectrum of disease severity (Table 1).

After quality control, 8022 MRI from healthy controls remained for the analyses and 107 MRI from patients with bvFTD, 44 MRI from patients with semantic dementia, and 38 MRI from patients with PNFA. We built our lifespan FTD models by combining MRI of patients with FTD with MRI of healthy controls because we assume that neurodegeneration is slow and progressive with smooth brain atrophy. Because 54 years was the maximum of the minimum age between FTD variants, we combined MRI of patients with FTD with 5699 MRI of healthy controls younger than 54 (all the subjects younger than 54 in the 8022 that were used for healthy aging models). In more detail, when building lifespan volumetric models for bvFTD, we used healthy controls for ages between 1 and 35; we mixed healthy controls and patients with bvFTD for ages between 35 and 54; and we used only patients with bvFTD for ages superior to 54. For semantic dementia models, we used healthy controls for age between 1 and 50, we mixed healthy controls and patients with semantic dementia for ages between 50 and 54; and we used only patients with semantic dementia for ages superior to 54. For PNFA models, we used healthy controls for ages between 1 and 54, and we used only patients with PNFA for ages superior to 54. Therefore, the parametric FTD models could be constrained over the entire lifespan.[25]

3.2 | Identification of brain structures diverging between healthy subjects and FTD variants trajectories

Figures S1 and S2 show, respectively, the 35 left brain structures and the 33 right brain structures (out of the 60 gray matter structures per hemisphere we have tested using AssemblyNet) that significantly diverged during lifespan between normal aging brain charts and at least one FTD variants. The three most affected structures over time (peak atrophy) were the right caudate, the right accumbens, and the left accumbens in bvFTD (distance between healthy aging model and bvFTD trajectory at 90 years old = 9.2, 8.8 and 8.4, respectively); the left inferior temporal gyrus, left accumbens, and left hippocampus in

Alzheimer's & Dementia®
THE JOURNAL OF THE ALZHEIMER'S ASSOCIATION

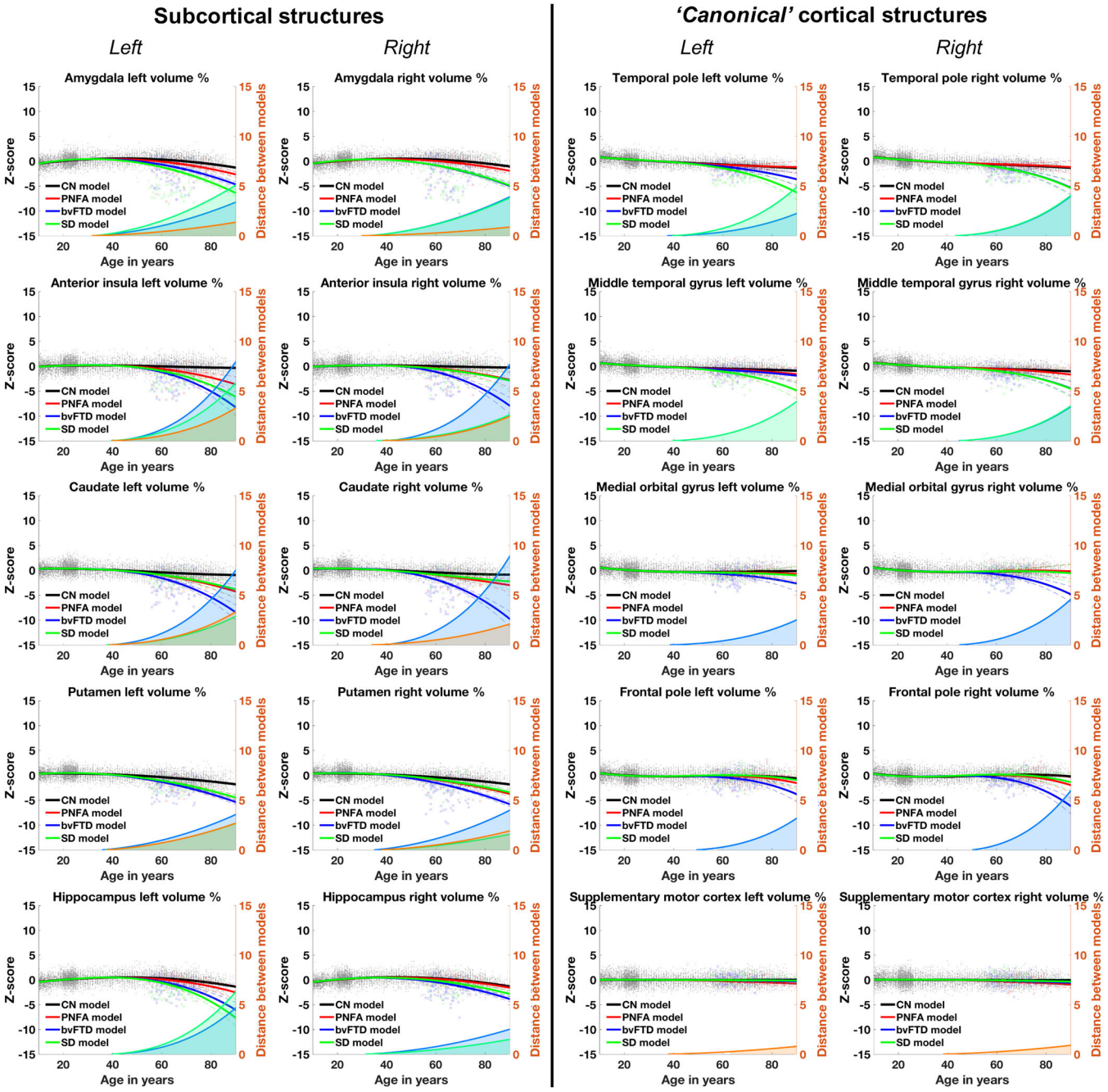

FIGURE 1 Lifespan trajectories based on z-scores of normalized brain volumes for CN subjects (in black) and the three FTD subtypes (bvFTD in blue, SD in green, and PNFA in red). Only the most relevant subcortical and "canonical" cortical structures (i.e. cortical regions involved in behavioral and/or language networks and usually described in FTD diagnostic criteria) are represented here (among 35 left brain structures and 33 right brain structures that significantly diverged during lifespan between normal aging brain charts and at least one FTD variants, see Figures S2 and S3). Black dots represent all healthy individuals and color dots FTD patients. The color curves represents the distance between the healthy and pathological models. The prediction bounds of the models are estimated with a confidence level at 95%. The blue (for bvFTD), green (for SD), and orange (for PNFA) areas indicate the time period where confidence intervals of both models do not overlap. bvFTD, behavioral variant of FTD; CN, cognitively normal; FTD, frontotemporal dementia; PNFA, progressive non-fluent aphasia; SD, standard deviation.

semantic dementia (distance = 8.1, 7.1, and 6.5); and the left accumbens, right accumbens, and left anterior insula in PNFA (distance = 4.2, 3.5, and 3.4). A total of 56 structures (left or right) were significantly smaller than controls in bvFTD, 33 in semantic dementia, and 25 in PNFA.

Figures S2 and S3 also showed that 22 brain structures were affected only in bvFTD (left and right [anterior, posterior, lateral, and medial] orbital gyrus, right inferior frontal gyrus, right middle frontal gyrus, left superior frontal gyrus, left and right medial frontal cortex, left and right frontal pole, right frontal operculum, right gyrus

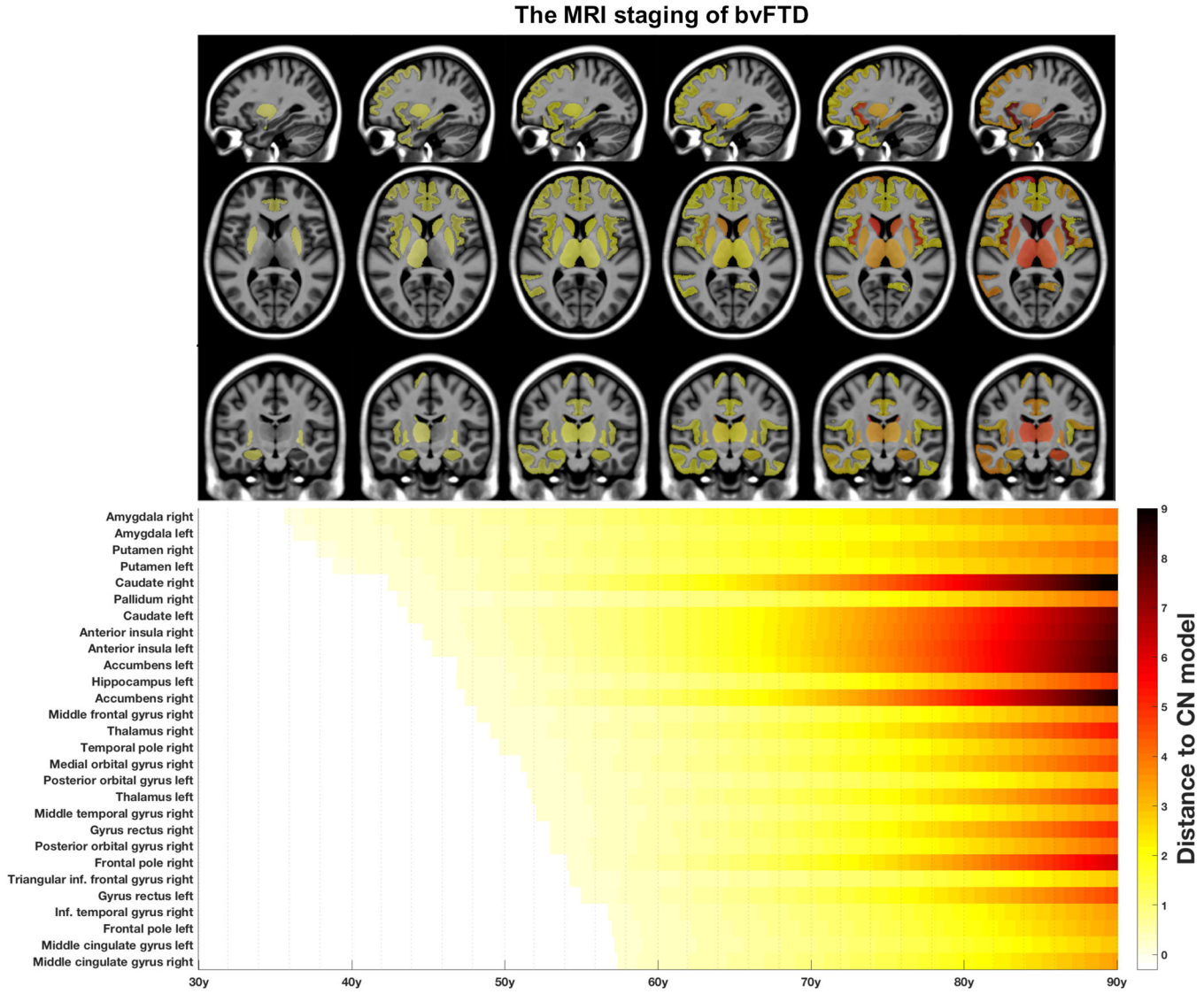

FIGURE 2 The MRI staging scheme of structural progression of bvFTD. The upper panel maps the progression of atrophy in the three axis (radiological convention, all brain structures identified in Figures S2 and S3). The lower panel is a timeline representing the sequential divergence of the most atrophic structures (top 50%) between healthy and bvFTD trajectories. The effect-size of structural divergence is color-coded according to the bar at the bottom right of the figure. bvFTD, behavioral variant of FTD.

rectus, left anterior cingulate gyrus, right middle cingulate gyrus, left and right pallidum, and right thalamus). Five structures were specifically affected in semantic dementia (left entorhinal cortex, left parahippocampal gyrus, left fusiform gyrus, left middle temporal gyrus, left superior temporal gyrus) and five in PNFA (left and right supplementary motor cortex, left parietal operculum, right precuneus, and right cuneus). *A contrario*, 13 brain structures were significantly affected in all three variants (bilateral amygdala, bilateral insula, bilateral accumbens, bilateral putamen, left caudate, left thalamus, left central operculum, left gyrus rectus, and right anterior cingulate gyrus).

We summarized these findings in Figure 1, where we present the most relevant subcortical and "canonical" cortical structures (i.e., cortical regions involved in behavioral and/or language networks and usually described in diagnostic criteria).

3.3 | MRI staging scheme of bvFTD, semantic dementia, and PNFA

We mapped in time and space on standardized brains the divergence of FTD variants volumetric trajectories from normal aging trajectories (upper panels in Figures 2, 3 and 4). For each FTD variant, we also built timelines highlighting the sequential divergence of the top 50% atrophic structures in bvFTD, semantic dementia, and PNFA (lower panel in Figures 2, 3, and 4). Schematically, when regrouping anatomical structures, five major stages of atrophy progression emerged in each FTD variant:

1. For bvFTD: (1) bilateral amygdala; (2) bilateral striatum; (3) bilateral anterior insula; (4) bilateral hippocampus and thalamus; and (5) right temporal pole and middle temporal gyrus, bilateral prefrontal

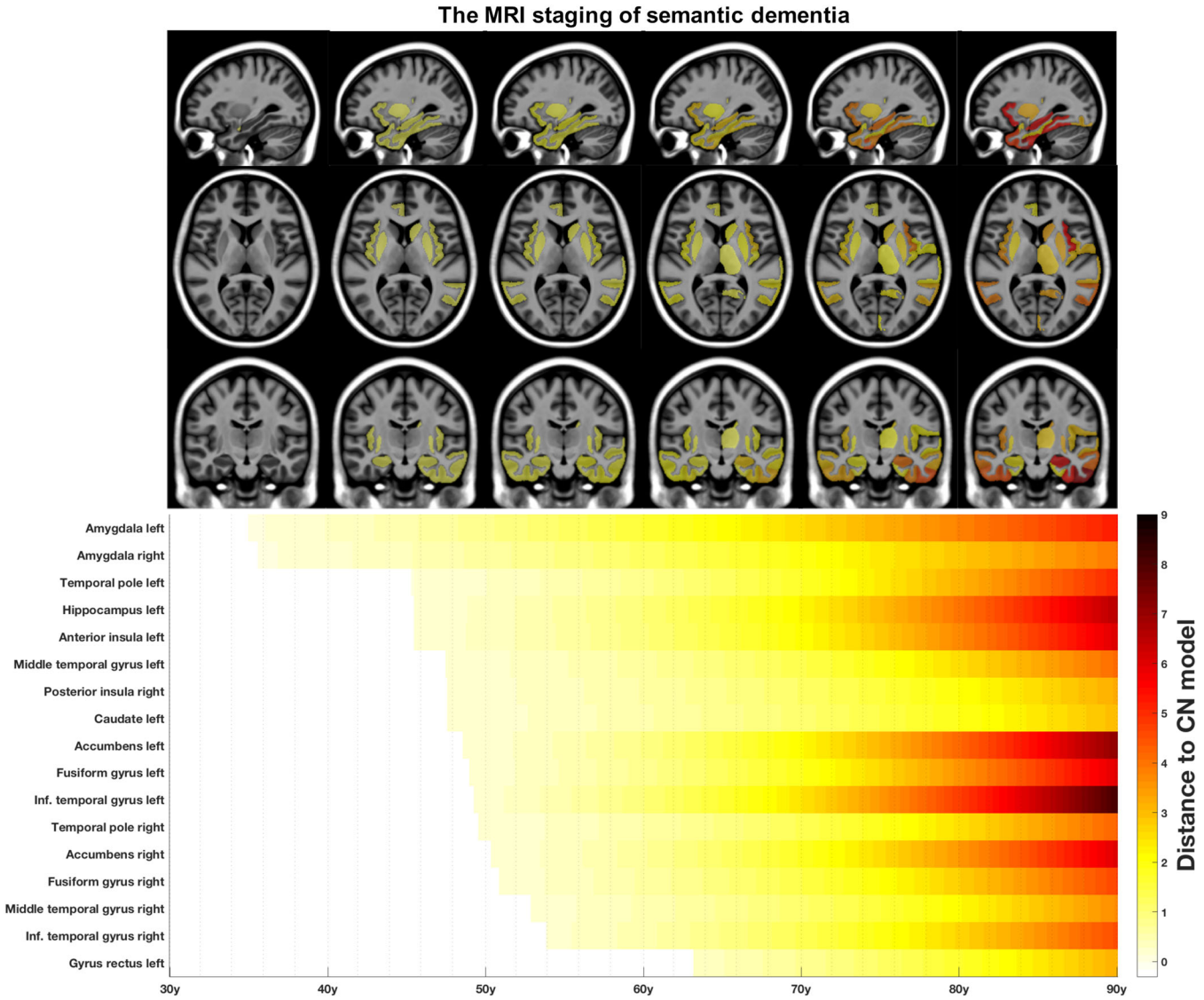

FIGURE 3 The MRI staging scheme of structural progression of semantic dementia. The upper panel maps the progression of atrophy in the three axis (radiological convention, all brain structures identified in Figures S2 and S3). The lower panel is a timeline representing the sequential divergence of the most atrophic structures (top 50%) between healthy and semantic dementia trajectories. The effect-size of structural divergence is color-coded according to the bar at the bottom right of the figure.

cortex (gyrus rectus, inferior frontal gyrus), orbital gyri, and frontal poles.

2. For semantic dementia: (1) bilateral amygdala; (2) left temporal pole, left hippocampus, and left anterior insula; (3) left middle temporal gyrus and striatum; (4) other left temporal structures; and (5) right-lateralization of temporal atrophy.
3. For PNFA: (1) left striatum; (2) bilateral anterior insula; (3) left thalamus; (4) left (and then right) operculum; and (5) left precuneus and cuneus.

In the three MRI staging schemes, subcortical atrophy precedes focal cortical atrophy in specific behavioral and/or language networks classically described in diagnostic criteria of bvFTD, semantic dementia, and PNFA.[5,6] These "radiological" prodromal phases can be measured as the time elapsed between the first significantly atrophied brain structure and the onset of the classical atrophy pattern. The "radiological" prodromal phase lasted 8 years in bvFTD (time between right amygdala atrophy and right insular atrophy), 10 years in semantic dementia (time between left amygdala atrophy and left temporal pole atrophy), and 8 years in PNFA (time between left putamen atrophy and left insular atrophy) (Figures 2, 3 and 4).

4 | DISCUSSION

In this study, we combined multiple large-scale MRI databases and whole-brain segmentation of fine-grained structures using a large ensemble of deep neural networks to describe the first exhaustive

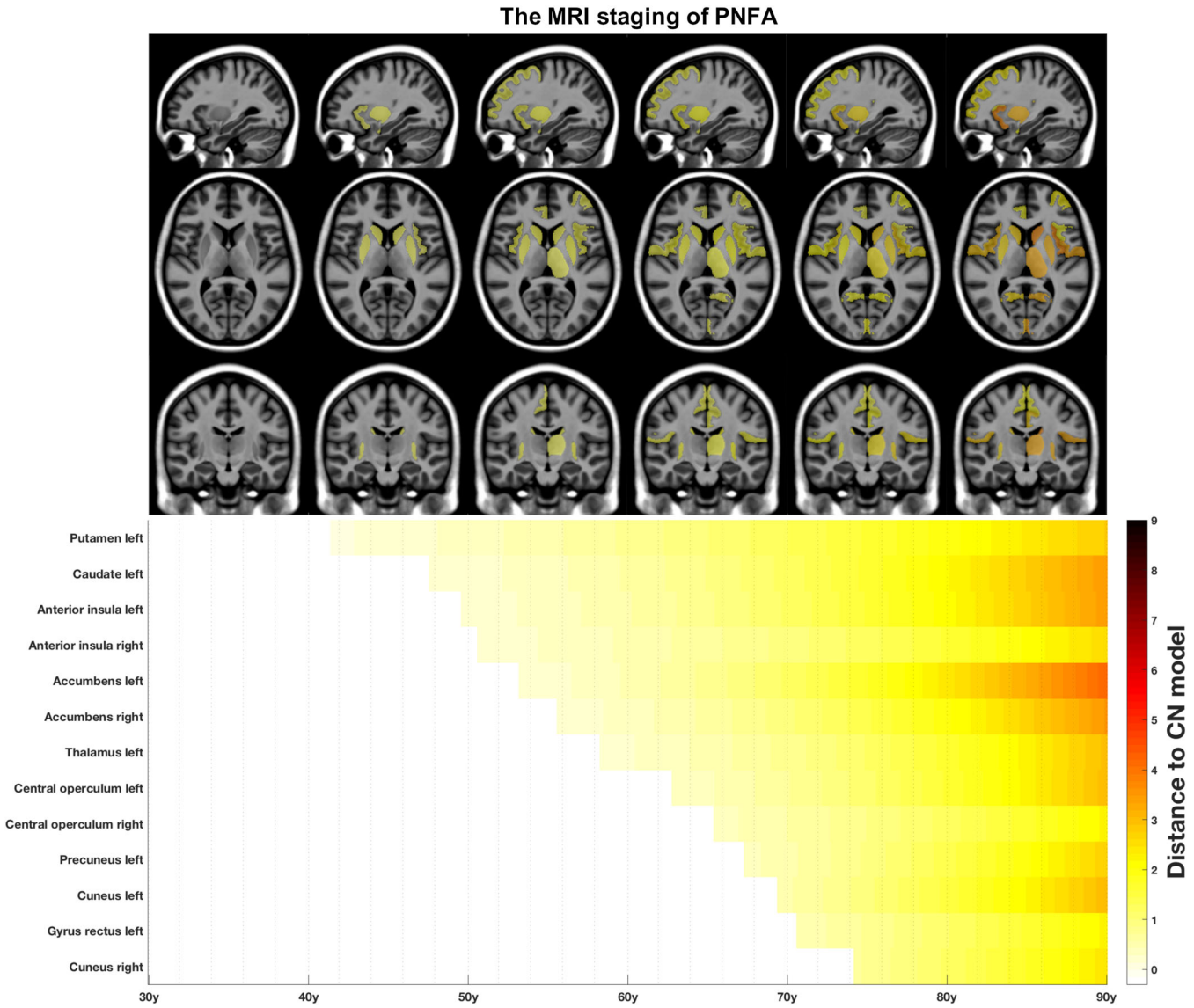

FIGURE 4 The MRI staging scheme of structural progression of PNFA. The upper panel maps the progression of atrophy in the three axis (radiological convention, all brain structures identified in Figures S2 and S3). The lower panel is a timeline representing the sequential divergence of the most atrophic structures (top 50%) between healthy and PNFA trajectories. The effect-size of structural divergence is color-coded according to the bar at the bottom right of the figure. PNFA, progressive non-fluent aphasia.

chronological structural progression of FTD variants over decades. We also described the differential severity of volumetric structure alterations. We found in all the three FTD variants that subcortical atrophy precedes focal cortical atrophy in specific behavioral and/or language networks. The canonical atrophy patterns of the three FTD variants appear relatively late during disease progression and there is a whole prodromal phase where subcortical atrophy predominates. In bvFTD, amygdalar and striatal atrophy precedes the fronto-temporo-insular atrophy described in diagnostic criteria.[5] Likewise, (bilateral) amygdalar atrophy precedes left temporo-polar atrophy in semantic dementia and left striatal atrophy precedes left fronto-insular (opercular) atrophy in PNFA.[6] We estimate that this "radiological" prodromal phase lasted 8 to 10 years. Furthermore, the most severely affected structures during the entire course of the three FTD variants are also these subcortical structures (and particularly the nucleus accumbens, in all three subtypes). Our results also show that in the later stages of FTD, a relative posterior extension of atrophy is possible, toward the precuneus and the cuneus (at least in PNFA). Atrophy is less severe and more circumscribed in PNFA than in bvFTD and semantic dementia.

Our findings using lifespan modeling in bvFTD are consistent with a recent meta-analysis of conventional transversal volumetric MRI studies where amygdala, striatum and anterior insula were among the structures most commonly reported to be affected compared to controls.[28] Outstanding subcortical involvement was also described in bvFTD using deformation-based morphometry[29] and was related to ventricular expansion, which can differentiate bvFTD and Alzheimer's disease.[30] In longitudinal MRI studies, greater rates of atrophy in the thalamus and the striatum were also reported in bvFTD compared to

Alzheimer's disease.[31] We report here that this subcortical pathological process is both early and severe during the course of bvFTD and is also found in semantic dementia and PNFA. These subcortical structures have many anatomical and functional connections with cortical areas. It will be interesting to test in future studies whether they may be differential "epicenters" of the pathological spreading of sporadic FTD variants,[32] because the neural network probably shapes atrophy patterns in FTD.[33]

Before full-blown FTD syndromes appear, our results suggest that first subtle cognitive, behavioral and/or language impairments may be linked to subcortical involvements rather than the "prototypical" or "canonical" cortical atrophy pattern described at the dementia stage.[34] Indeed, the striatum, the insula, and the amygdala are known to be involved in reward processing and motivation.[35] Within the striatum, the important vulnerability of the nucleus accumbens in all three subtypes is for instance an interesting anatomical correlate of apathy and impulsivity that can be found in every FTD variant.[36] Our results are also in line with a recent study showing that patients with bvFTD or semantic dementia exhibit early anhedonia, associated with insular and striatal atrophy.[37] The subcortical prodromal phase of atrophy, associated with early anhedonia, apathy, or impulsivity are potential early markers of FTD for future imaging-supported diagnostic criteria.

The NIFD and NACC imaging databases used in the present study included sporadic forms of FTD (or patients with unknown genetic background). However, our findings interestingly echo recent anatomical work in presymptomatic carriers of FTD-causative mutations where massive atrophy was described in subcortical structures up to 20 years before disease onset.[9,10,11,12] Subcortical atrophy might be more important in *C9orf72* carriers than in *MAPT* or *GRN* mutation carriers, with a particular vulnerability of the thalamus and to a lesser extent, the amygdala.[38] Our methodological approach to describe the preclinical and prodromal stages of FTD variants at the anatomical level using brain charts is complementary to these articles focusing on morphological brain changes in presymptomatic FTD-mutation carriers. In these cohorts of genetic FTD, it will be interesting to investigate whether early subcortical atrophy explain the distinct temporal progression patterns of cortical atrophy recently identified using machine-learning (Subtype and Stage Inference, SuStaIn).[39]

One of the strength of our study is to assess the volumetric progression of FTD variants at the whole-brain level, with a full screening of the diverging brain areas across lifespan between healthy subjects and patients with sporadic FTD. Our methodological approach offers new pathophysiological insights compared to the traditional longitudinal MRI analyzes that only cover heterogeneous and limited periods of disease development. An important advantage of our approach is also to provide standardized effect-sizes to quantify neuroanatomical divergence (i.e., atrophy) between healthy subjects and patients with FTD. Furthermore, our study compare "back-to-back" bvFTD, semantic dementia, and PNFA, identifying both in time and space the similarities and anatomical differences between FTD variants. For instance, we have shown that early subcortical atrophy was common to all FTD syndromes but that 22 brain structures were specifically affected in bvFTD, 5 specifically in semantic dementia, and 5 specifically in PNFA. These specific anatomical damages are intimately correlated to the definition of these clinical syndromes.[6]

We hope that these three MRI staging schemes will help in the early diagnosis of patients and that they will change the current paradigm according to which diagnostic MRI is frequently considered "negative" at early stages in FTD.[40] Beyond the anatomical description that we report here, it will be interesting in the near future to develop a novel framework for automatic FTD detection using normative and pathological lifespan models, as we previously did for Alzheimer's disease with the hippocampal-amygdalo-ventricular atrophy score.[41]

Regarding the limitations of this study, we regret the absence of a group with right temporal FTD, but this fourth variant of FTD is still equivocal and not present in current international diagnostic criteria.[42] Therefore, it is not listed in databases such as NACC and NIFD. We also acknowledge the lack of genetic or neuropathological information regarding the patients included in our brain charts of FTD variants. It prevents us from drawing conclusions about correlations between atrophy progression and neuropathology (tau or TDP-43 proteinopathies). Thus, the MRI staging presented here must be seen as the "average" anatomical staging of FTD clinical syndromes and not as an aetiologic/pathologic staging of frontotemporal lobar degenerations.[1] Furthermore, it is important to stress that these three MRI staging schemes only represent lifespan models of brain atrophy in FTD, but not models of clinical progression. Moreover, we must keep in mind that the pathological dynamic volumetric trajectories reported here are based on cross-sectional MRI collected on symptomatic patients with mild cognitive/behavioral impairment or dementia. Although we have previously validated this methodology over limited periods covered by longitudinal data in Alzheimer's disease,[16] our findings can still be considered preliminary, and grounds for future studies in FTD.

To conclude, we have modeled the global structural progression of bvFTD, semantic dementia, and PNFA over the entire course of these diseases. We found that in all three FTD variants, subcortical atrophy precede focal cortical atrophy in specific behavioral and/or language networks. Amygdalar and striatal atrophy may be the anatomical correlates of early cognitive, behavioral, and/or language impairments and may be good candidate biomarkers for future definitions of preclinical and prodromal FTD syndromes.

ACKNOWLEDGMENTS

The C-MIND data used in the preparation of this article were obtained from the C-MIND Data Repository created by the C-MIND study of Normal Brain Development. A listing of the participating sites and a complete listing of the study investigators can be found at https://research.cchmc.org/c-mind. The NDAR data used in the preparation of this manuscript were obtained from the NIH-supported National Database for Autism Research (NDAR). This is supported by the National Institute of Child Health and Human Development, the National Institute on Drug Abuse, the National Institute of Mental Health, and the National Institute of Neurological Disorders and Stroke. A listing of the participating sites and a complete listing of the

study investigators can be found at https://pediatricmri.nih.gov/nihpd/info/participating_centers.html. The ICBM data used in the preparation of this manuscript were supported by Human Brain Project grant PO1MHO52176-11 and Canadian Institutes of Health Research grant MOP- 34996. The IXI data used in the preparation of this manuscript were supported by the U.K. Engineering and Physical Sciences Research Council (EPSRC) GR/S21533/02 - https://www.brain-development.org/. The ABIDE data used in the preparation of this manuscript were supported by ABIDE funding resources listed at ht tps://fcon_1000.projects.nitrc.org/indi/abide/. The ADNI data used in the preparation of this manuscript were obtained from the Alzheimer's Disease Neuroimaging Initiative (ADNI) (National Institutes of Health Grant U01 AG024904). The ADNI is funded by the National Institute on Aging and the National Institute of Biomedical Imaging and Bioengineering and through generous contributions from private partners as well as nonprofit partners listed at: https://ida.loni.usc.edu/collaboration/access/appLicense.jsp. Private sector contributions to the ADNI are facilitated by the Foundation for the National Institutes of Health (www.fnih.org). The grantee organization is the Northern California Institute for Research and Education, and the study was coordinated by the Alzheimer's Disease Cooperative Study at the University of California, San Diego. ADNI data are disseminated by the Laboratory for NeuroImaging at the University of California, Los Angeles. This research was also supported by NIH grants P30AG010129, K01 AG030514 and the Dana Foundation. The AIBL data used in the preparation of this manuscript were obtained from the AIBL study of ageing funded by the Common-wealth Scientific Industrial Research Organization (CSIRO; a publicly funded government research organization), Science Industry Endowment Fund, National Health and Medical Research Council of Australia (project grant 1011689), Alzheimer's Association, Alzheimer's Drug Discovery Foundation, and an anonymous foundation. See www.aibl.csiro.au for further details. The ADHAD, DLBS and SALD data used in the preparation of this article were obtained from ht tps://fcon_1000.projects.nitrc.org (Mennes M et al., NeuroImage, 2013; Wei D et al., bioRxiv 2017). The ISYB data were download from https://www.scidb.cn (Imaging Chinese Young Brains, https://doi.org/10.11922/sciencedb.00740). Data used in the preparation of this article were also obtained from the MIRIAD database (Malone IB et al., NeuroImage, 2012) The MIRIAD investigators did not participate in analysis or writing of this report. The MIRIAD dataset is made available through the support of the UK Alzheimer's Society (Grant RF116). The original data collection was funded through an unrestricted educational grant from GlaxoSmithKline (Grant 6GKC). Data used in the preparation of this article were obtained from the Parkinson's progression Markers Initiative (PPMI) database (www.ppmi-info.org). PPMI – a public-private partnership – was funded by The Michael J. Fox Foundation for Parkinson's Research and funding partners that can be found at https://www.ppmi-info.org/about-ppmi/who-we-are/study-sponsors. The Amsterdam open MRI collection AOMIC ID-1000/PIOP1/PIOP2 data used in the preparation of this article were obtained from https://nilab-uva.github.io/AOMIC.github.io/ (Snoek L et al., Scientific data, 2021). The Calgary preschool MRI dataset was available at https://osf.io/axz5r/ and supported by University of Calgary and CIHR (IHD-134090 & MOP-136797). Data collection and sharing for this project was provided by the Cambridge Centre for Ageing and Neuroscience (CamCAN, https://camcan-archive.mrc-cbu.cam.ac.uk/dataaccess/). CamCAN funding was provided by the UK Biotechnology and Biological Sciences Research Council (grant number BB/H008217/1), together with support from the UK Medical Research Council and University of Cambridge, UK. The Pixar database and related fundings were available at https://openneuro.org/datasets/ds000228/versions/1.1.0 (Richardson H et al., Nat Commun, 2018). Data used in the preparation of this work were obtained from the DecNef Project Brain Data Repository (https://bicr-resource.atr.jp/srpbsopen/) gathered by a consortium as part of the Japanese Strategic Research Program for the Promotion of Brain Science (SRPBS) supported by the Japanese Advanced Research and Development Programs for Medical Innovation (AMED, Tanaka SC et al., Scientific data, 2021). FTLDNI was funded through the National Institute of Aging, and started in 2010. The primary goals of FTLDNI were to identify neuroimaging modalities and methods of analysis for tracking frontotemporal lobar degeneration (FTLD) and to assess the value of imaging versus other biomarkers in diagnostic roles. The Principal Investigator of NIFD was Dr. Howard Rosen, MD, at the University of California, San Francisco. The data are the result of collaborative efforts at three sites in North America. For up-to-date information on participation and protocol, please visit http://memory.ucsf.edu/research/studies/nifd. Data collection and sharing for this project was funded by the Frontotemporal Lobar Degeneration Neuroimaging Initiative (National Institutes of Health Grant R01 AG032306). The study is coordinated through the University of California, San Francisco, Memory and Aging Center. FTLDNI data are disseminated by the Laboratory for Neuro Imaging at the University of Southern California. The NACC database was funded by NIA/NIH Grants listed at https://naccdata.org/publish-project/authors-checklist#acknowledgment.

We thank all investigators of these projects who collected these datasets and made them freely accessible. This manuscript reflects the views of the authors and may not reflect the opinions or views of the database providers.

This work benefited from the support of the project DeepVolBrain of the French National Research Agency (ANR-18-CE45-0013). This study was achieved within the context of the Laboratory of Excellence TRAIL ANR-10-LABX-57 for the BigDataBrain project. Moreover, we thank the Investments for the future Program IdEx Bordeaux (ANR-10-IDEX-03-02 and RRI "IMPACT"), the French Ministry of Education and Research, and the CNRS for DeepMultiBrain project. This study has also been supported by the PID2020-118608RB-I00 grants from the Spanish Ministerio de Ciencia e innovación. The sponsors did not participate in any aspect of the design or performance of the study, including data collection, management, analysis, and the interpretation or preparation, review, and approval of the manuscript.

CONFLICT OF INTEREST STATEMENT

The authors declare no competing financial interests relative to the present study. Author disclosures are available in the supporting information.

REFERENCES

1. Boeve BF, Boxer AL, Kumfor F, Pijnenburg Y, Rohrer JD. Advances and controversies in frontotemporal dementia: diagnosis, biomarkers, and therapeutic considerations. *Lancet Neurol*. 2022;21:258-272. doi:10.1016/S1474-4422(21)00341-0
2. Barker MS, Gottesman RT, Manoochehri M, et al. Proposed research criteria for prodromal behavioural variant frontotemporal dementia. *Brain*. 2022;145:1079-1097. doi:10.1093/brain/awab365
3. Villain N, Planche V, Levy R. High-clearance anti-amyloid immunotherapies in Alzheimer's disease. Part 1: meta-analysis and review of efficacy and safety data, and medico-economical aspects. *Rev Neurol (Paris)*. 2022;178:1011-1030. doi:10.1016/j.neurol.2022.06.012
4. Harper L, Barkhof F, Scheltens P, Schott JM, Fox NC. An algorithmic approach to structural imaging in dementia. *J Neurol Neurosurg Psychiatry*. 2014;85:692-698. doi:10.1136/jnnp-2013-306285
5. Rascovsky K, Hodges JR, Knopman D, et al. Sensitivity of revised diagnostic criteria for the behavioural variant of frontotemporal dementia. *Brain*. 2011;134:2456-2477. doi:10.1093/brain/awr179
6. Gorno-Tempini ML, Hillis AE, Weintraub S, et al. Classification of primary progressive aphasia and its variants. *Neurology*. 2011;76:1006-1014. doi:10.1212/WNL.0b013e31821103e6
7. Rogalski E, Cobia D, Martersteck A, et al. Asymmetry of cortical decline in subtypes of primary progressive aphasia. *Neurology*. 2014;83:1184-1191. doi:10.1212/WNL.0000000000000824
8. Harper L, Bouwman F, Burton EJ, et al. Patterns of atrophy in pathologically confirmed dementias: a voxelwise analysis. *J Neurol Neurosurg Psychiatry*. 2017;88:908-916. doi:10.1136/jnnp-2016-314978
9. Bertrand A, Wen J, Rinaldi D, et al. Early cognitive, structural, and microstructural changes in presymptomatic C9orf72 carriers younger than 40 years. *JAMA Neurol*. 2018;75:236-245. doi:10.1001/jamaneurol.2017.4266
10. Lee SE, Sias AC, Mandelli ML, et al. Network degeneration and dysfunction in presymptomatic C9ORF72 expansion carriers. *Neuroimage Clin*. 2017;14:286-297. doi:10.1016/j.nicl.2016.12.006
11. Papma JM, Jiskoot LC, Panman JL, et al. Cognition and gray and white matter characteristics of presymptomatic C9orf72 repeat expansion. *Neurology*. 2017;89:1256-1264. doi:10.1212/WNL.0000000000004393
12. Bocchetta M, Todd EG, Peakman G. Differential early subcortical involvement in genetic FTD within the GENFI cohort. *Neuroimage Clin*. 2021;30:102646. doi:10.1016/j.nicl.2021.102646
13. Staffaroni AM, Ljubenkov PA, Kornak J, et al. Longitudinal multimodal imaging and clinical endpoints for frontotemporal dementia clinical trials. *Brain*. 2019;142:443-459. doi:10.1093/brain/awy319
14. Coupé P, Catheline G, Lanuza E, Manjón JV. Alzheimer's disease neuroimaging initiative. Towards a unified analysis of brain maturation and aging across the entire lifespan: a MRI analysis. *Hum Brain Mapp*. 2017;38:5501-5518. doi:10.1002/hbm.23743
15. Bethlehem R A I, Seidlitz J, White SR, et al. Brain charts for the human lifespan. *Nature*. 2022;604:525-533. doi:10.1038/s41586-022-04554-y
16. Planche V, Manjon JV, Mansencal B, et al. Structural progression of Alzheimer's disease over decades: the MRI staging scheme. *Brain Commun*. 2022;4:fcac109. doi:10.1093/braincomms/fcac109
17. Coupé P, Mansencal B, Clément M, et al. AssemblyNet: a large ensemble of CNNs for 3D whole brain MRI segmentation. *Neuroimage*. 2020;219:117026. doi:10.1016/j.neuroimage.2020.117026
18. Manjón JV, Coupé P, Martí-Bonmatí L, Collins DL, Robles M. Adaptive non-local means denoising of MR images with spatially varying noise levels. *J Magn Reson Imaging*. 2010;31:192-203. doi:10.1002/jmri.22003
19. Manjón JV, Tohka J, Robles M. Improved estimates of partial volume coefficients from noisy brain MRI using spatial context. *Neuroimage*. 2010;53:480-490. doi:10.1016/j.neuroimage.2010.06.046
20. Tustison NJ, Avants BB, Cook PA, et al. N4ITK: improved N3 bias correction. *IEEE Trans Med Imaging*. 2010;29:1310-1320. doi:10.1109/TMI.2010.2046908
21. Avants BB, Tustison NJ, Song G, Cook PA, Klein A, Gee JC. A reproducible evaluation of ANTs similarity metric performance in brain image registration. *Neuroimage*. 2011;54:2033-2044. doi:10.1016/j.neuroimage.2010.09.025
22. Manjón JV, Tohka J, García-Martí G, et al. Robust MRI brain tissue parameter estimation by multistage outlier rejection. *Magn Reson Med*. 2008;59:866-873. doi:10.1002/mrm.21521
23. Manjón JV, Romero JE, Vivo-Hernando R, et al. Deep ICE: a deep learning approach for MRI Intracranial Cavity Extraction *arXiv: Quantitative Methods*. 2020. doi:https://arXiv.2001.05720
24. Denis de Senneville B, Manjón JV, Coupé P. RegQCNET: deep quality control for image-to-template brain MRI affine registration. *Phys Med Biol*. 2020;65:225022. doi:10.1088/1361-6560/abb6be
25. Coupé P, Manjón JV, Lanuza E, Catheline G. Lifespan changes of the human brain in Alzheimer's disease. *Sci Rep*. 2019;9:3998. doi:10.1038/s41598-019-39809-8
26. Klein A, Tourville J. 101 labeled brain images and a consistent human cortical labeling protocol. *Front Neurosci*. 2012;6:171. doi:10.3389/fnins.2012.00171
27. Knol MJ, Pestman WR, Grobbee DE. The (mis)use of overlap of confidence intervals to assess effect modification. *Eur J Epidemiol*. 2011;26:253-254. doi:10.1007/s10654-011-9563-8
28. Kamalian A, Khodadadifar T, Saberi A, et al. Convergent regional brain abnormalities in behavioral variant frontotemporal dementia: a neuroimaging meta-analysis of 73 studies. *Alzheimers Dement (Amst*. 2022;14:e12318. doi:10.1002/dad2.12318
29. Manera AL, Dadar M, Collins DL, Ducharme S. Frontotemporal Lobar Degeneration Neuroimaging Initiative. Deformation based morphometry study of longitudinal MRI changes in behavioral variant frontotemporal dementia. *Neuroimage Clin*. 2019;24:102079. doi:10.1016/j.nicl.2019.102079
30. Manera AL, Dadar M, Collins DL, Ducharme S, Frontotemporal Lobar Degeneration Neuroimaging Initiative (FTLDNI), Alzheimer's Disease Neuroimaging Initiative (ADNI). Ventricular features as reliable differentiators between bvFTD and other dementias. *Neuroimage Clin*. 2022;33:102947. doi:10.1016/j.nicl.2022.102947
31. Landin-Romero R, Kumfor F, Leyton CE, Irish M, Hodges JR, Piguet O. Disease-specific patterns of cortical and subcortical degeneration in a longitudinal study of Alzheimer's disease and behavioural-variant frontotemporal dementia. *Neuroimage*. 2017;151:72-80. doi:10.1016/j.neuroimage.2016.03.032
32. Brown JA, Deng J, Neuhaus J, et al. Patient-tailored, connectivity-based forecasts of spreading brain atrophy. *Neuron*. 2019;104:856-868.e5. doi:10.1016/j.neuron.2019.08.037
33. Shafiei G, Bazinet V, Dadar M, et al. Network structure and transcriptomic vulnerability shape atrophy in frontotemporal dementia. *Brain*. 2023;146(1):321-336. doi:10.1093/brain/awac069
34. Rohrer JD. Structural brain imaging in frontotemporal dementia. *Biochim Biophys Acta*. 2012;1822:325-332. doi:10.1016/j.bbadis.2011.07.014
35. Levy R, Dubois B. Apathy and the functional anatomy of the prefrontal cortex-basal ganglia circuits. *Cereb Cortex*. 2006;16:916-928. doi:10.1093/cercor/bhj043
36. Basar K, Sesia T, Groenewegen H, Steinbusch HWM, Visser-Vandewalle V, Temel Y. Nucleus accumbens and impulsivity. *Prog Neurobiol*. 2010;92:533-557. doi:10.1016/j.pneurobio.2010.08.007
37. Shaw SR, El-Omar H, Roquet D, et al. Uncovering the prevalence and neural substrates of anhedonia in frontotemporal dementia. *Brain*. 2021;144:1551-1564. doi:10.1093/brain/awab032

38. Saracino D, Le Ber I. How can we define the presymptomatic C9orf72 disease in 2022? An overview on the current definitions of preclinical and prodromal phases. *Rev Neurol (Paris)*. 2022;178:426-436. doi:10.1016/j.neurol.2022.03.007
39. Young AL, Marinescu RV, Oxtoby NP, et al. Uncovering the heterogeneity and temporal complexity of neurodegenerative diseases with subtype and stage inference. *Nat Commun*. 2018;9:4273. doi:10.1038/s41467-018-05892-0
40. Mesulam M-M, Wieneke C, Thompson C, Rogalski E, Weintraub S. Quantitative classification of primary progressive aphasia at early and mild impairment stages. *Brain*. 2012;135:1537-1553. doi:10.1093/brain/aws080
41. Coupé P, Manjón JV, Mansencal B, Tourdias T, Catheline G, Planche V. Hippocampal-amygdalo-ventricular atrophy score: alzheimer disease detection using normative and pathological lifespan models. *Hum Brain Mapp*. 2022;43:3270-3282. doi:10.1002/hbm.25850
42. Ulugut Erkoyun H, Groot C, Heilbron R, et al. A clinical-radiological framework of the right temporal variant of frontotemporal dementia. *Brain*. 2020;143:2831-2843. doi:10.1093/brain/awaa225

SUPPORTING INFORMATION

Additional supporting information can be found online in the Supporting Information section at the end of this article.

How to cite this article: Planche V, Mansencal B, Manjon JV, Tourdias T, Catheline G, Coupé P. Anatomical MRI staging of frontotemporal dementia variants. *Alzheimer's Dement*. 2023;19:3283–3294. https://doi.org/10.1002/alz.12975